Energy Conversion and Management 295 (2023) 117634

Contents lists available at ScienceDirect

Energy Conversion and Management

journal homepage: www.elsevier.com/locate/enconman

Field-test performance models of a residential micro-cogeneration system based on the hybridization of a proton exchange membrane fuel cell and a gas condensing boiler

Nicolas Paulus *, Vincent Lemort

Thermodynamics Laboratory, University of Liège, Allée de la découverte 17, 4000 Liège, Belgium

ARTICLE INFO

Keywords:
Fuel cell
Micro-cogeneration
Modelling
Efficiency
Hybridization
Goodness of fit

ABSTRACT

The energy transition brings focus on cogeneration systems, even at residential levels. One of the latter systems consists in a proton exchange membrane fuel cell (PEMFC) combined with a gas condensing boiler and a 220L domestic hot water tank. The system, fed by natural gas, is designed to provide the heat demands of residential houses and to participate locally in the electrical production thanks to the PEMFC of nominal constant power of 0.75kW$_{el}$ (and 1.1kW$_{th}$). The boiler, sized for peak heat demands, can be chosen between four rated power versions from 11.4 to 30.8kW$_{th}$. The machine is never electrically driven. This study has developed daily (and monthly) performance models of the system based on field-test results of two machines installed and monitored in Belgium for the whole year 2020. All models only require daily (or monthly) heat demands of the building as inputs but more elaborated (and accurate) models have been established considering operating temperatures and the demonstrated ability of the machine to modulate its heat rate output in real onsite applications. Finally, this paper has demonstrated that the daily PEMFC load factor (its daily electrical production) has a significant influence on the daily performance and therefore on the goodness of fit of the models. Unfortunately, the demonstrated PEMFC load factor is unexpectedly low for the monitored dwellings, probably due to the high level of complexity of the hybridization between the components of the system.

1. Introduction

The Intergovernmental Panel on Climate Change (IPCC) recently released its Sixth Assessment Report in April 2022, which stated that in order to keep global warming below 2 °C compared to preindustrial temperatures, humanity can emit a maximum of 890 GtCO$_2$ from January 1st, 2020 [1]. This means that even at the residential level, efforts to mitigate greenhouse gas emissions are necessary, with a focus on using cleaner power sources and combined heat and power (CHP) systems, such as fuel cells. Also, those systems usually do not emit other harmful pollutants often involved in the combustion of hydrocarbons, such as SO_2 and NO_x [2]. One such system, which has already been commercialized and tested in independent laboratories [3], is made up of a natural gas-fed proton exchange membrane fuel cell (PEMFC) that generates a constant electrical power of 0.75 kW$_{el}$, combined with a gas condensing boiler and a domestic hot water (DHW) tank. The PEMFC is not always producing electricity as it is reported in its datasheet that it shuts down if it can no longer dissipate its heat in the space heating or in the DHW tank and that its return temperature reaches 50 °C.

Two of those systems, installed in different houses in Belgium, were completely monitored for the whole year 2020. Based on that monitoring data, the aim of this paper is to provide simple performance models of the CHP system that could easily be used in building performance simulation studies. Contrary to models based on laboratory studies or on the datasheet figures, the main advantage of the models developed in this work is that they are based on real all year long field-test performance. Unoptimized operating conditions, that could potentially come from the way the owner uses the system or the way it has been installed in the building, are very likely to occur in real applications. Those sources of inefficiency are involved in the field-test data considered in the models of this work, making them therefore more realistic than a model solely based on laboratory testing in ideal conditions.

This paper first offer two simple single-variable time-invariant [4] models that provide the daily (or monthly) thermal efficiency of the system with only one input: the total daily (or monthly) heat demand of

* Corresponding author.
E-mail addresses: nicolas.paulus@uliege.be, nicolas.paulus@hepl.be (N. Paulus), vincent.lemort@uliege.be (V. Lemort).

https://doi.org/10.1016/j.enconman.2023.117634
Received 24 April 2023; Received in revised form 25 July 2023; Accepted 4 September 2023
Available online 10 September 2023

the buildings, which thus considers the addition of the domestic hot water (DHW) demand and the space heating demand. The daily-based model is subsequently improved considering other parameters influencing the daily thermal efficiency. Firstly, the efficiency of space heating appliances is indeed known to be enhanced at lower operating temperatures [5]. Secondly, transient effect and unsmooth heat demand are known to lessen the thermal efficiency of space heating appliances [6]. Thanks to the monitoring data, both effects will be considered in the enhanced single-variable time-invariant models by implementing specifically defined correction factors. If a potential user of those models has an idea of the operating temperatures and/or of the smoothness of the heat demand that will occur in the building he is considering, he will have a more accurate estimation of the daily thermal efficiency of the system.

It has then been observed that the daily electrical production of the system (which is part of the monitoring data), or more generally, the load factor of the PEMFC, has a significant influence on the thermal efficiency of the whole system. Therefore, two-variable models (daily heat demand and daily electrical production or daily PEMFC load factor) are thus offered in this work. They provide the best estimate of the daily thermal efficiency of the system but the PEMFC load factor is unfortunately not easily estimated for potential users of those models. At last, knowing the daily PEMFC load factor (or its daily electrical production), the daily electrical efficiency can be computed for each of the models of this work.

2. Material and methods

2.1. The system

The residential micro-cogeneration modelled in this work is the same in both studied houses and its internal schematics is presented in Fig. 1 (a) [7]. Its main performance targets, declared by the OEM (Original Equipment Manufacturer) and expressed in Low Heating Value (LHV) are shown in Table 1 and Fig. 1 (b) [7]. It has been designed to cope with a wide range of residential space heating applications (with the maximum heat rate output of 30.8 kW_{th}).

Table 1
PEMFC gas boiler hybrid expected targets.

Datasheet figures	Values
Maximum electrical production a day	17 kWh_{el}
Fuel cell rated electrical & heat rate output	0.75 kW_{el} & 1.1 kW_{th}
Electrical LHV efficiency of the PEMFC only	37 %
Max global Fuel cell LHV efficiency	92 %
Max boiler efficiency (at rated power) [1]	108.6 %
Condensing gas boiler nominal heat rate outputs (4 versions)	11.4 |19.0 | 24.5 | 30.8kW_{th}

[1] Considering HHV to LHV ratio of 1.1085 [14].

As mentioned, the system is fed by natural gas (high methane proportion). It involves an upstream "external" reformer before the PEMFC as temperature within the stack is not sufficiently high for direct "internal" reforming at the electrode [8], which is frequent for solid oxide fuel cells [9]. The hydrogen production is instantaneous (and simultaneous to the power production of the PEMFC) so the system is not subjected to the highly constraining safety issues regarding hydrogen storage such as the ICPE (Installation Classée pour la Protection de l'Environnement) authorization in France or similar other legal barriers on EU markets [10]. Reforming technology has not been officially disclosed in the datasheet but a previous study allows for assuming that the very frequent methane steam reforming reaction does occur in this case [11]. Further information on the assumed reforming system, reaction and processes occurring in this particular system have been previously studied [12] and it can indeed be assumed that hydrogen is produced mainly by steam reforming (and/or partial oxidation of methane) [13].

This particular fuel cell operates in a 48-hour cycle: continuous constant electrical production for a maximum of 45.5 h (if heat dissipation to the tank or to the space heating is sufficient) followed by a 2.5-hour "recovery" phase (as the OEM calls it) for which the PEMFC has to be shut down. This is the reason why maximum electrical production has

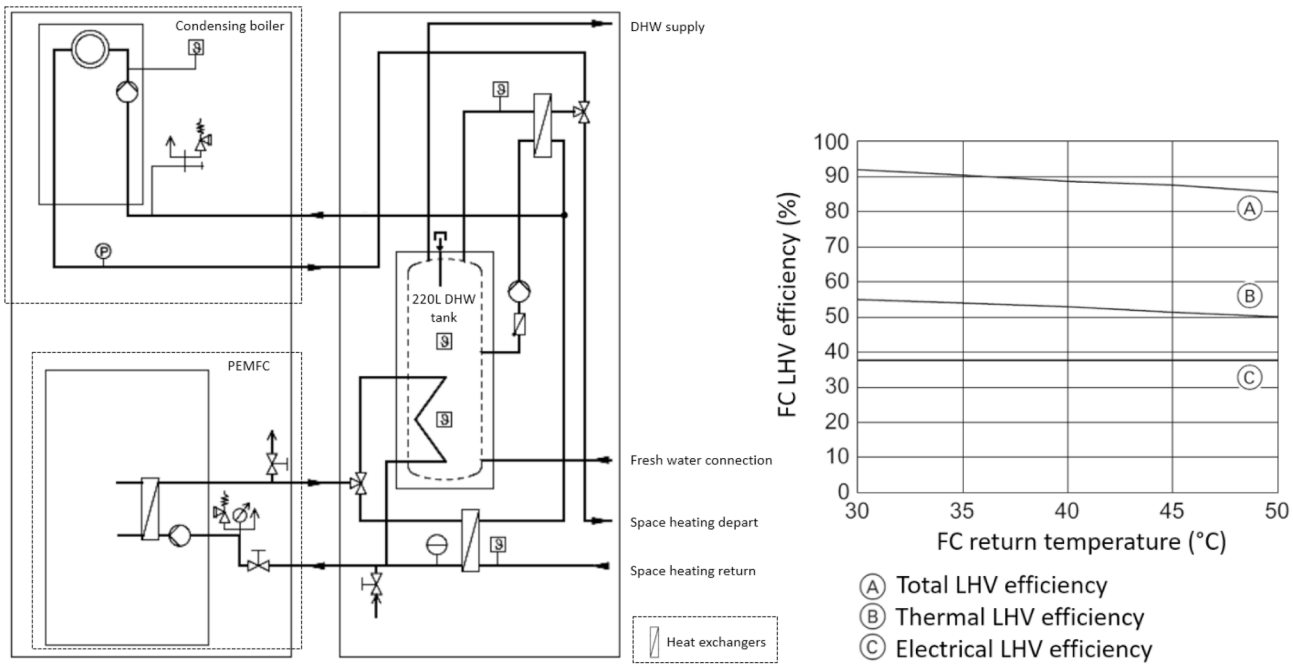

(a) (b)

Fig. 1. (**a**) System's architecture: high level of integration (through two heat exchangers, several 3-way valves and several pumps) of the PEMFC with the gas condensing boiler and the DHW tank [7]. The PEMFC and gas boiler can either run separately or simultaneously.; (**b**) OEM's declared LHV efficiency for the PEMFC system only [7].

been declared in Table 1 to "only" 17 kWh_{el} and not to 18 kWh_{el} (which would have corresponded to the fuel cell rated electrical power). The OEM has not disclosed what is specifically intended with this "recovery" phase. However, a parallel study conducted by the authors of this work concluded that it most likely consists in ammonia poisoning removal for the regeneration of the selective oxidation catalyst [12]. This selective oxidation process [15] is used in the reforming system to eliminate carbon monoxide [16], or at least reduce its concentration to acceptable levels of about 5 ppm [17], because it is known to be extremely harmful to the PEMFC core components [18]. It is worth mentioning that it is not excluded that other degradation mechanisms of PEMFC are also aimed with this "recovery" phase, such as, for example, the lowered oxygen reduction reaction kinetics at the cathode, usually caused by oxidation, dissolution [19] and sintering (redeposition mechanism of crystallite growth) [20] of the platinum catalyst, commonly used to significantly enhance the rate of the reduction reaction [21].

2.2. The monitored houses

The PEMFC – gas boiler hybrid system presented here above has been monitored in-situ, in two real households in Belgium, for the whole year 2020. The first house is located in Huy whereas the other one is located in Oostmalle. From a climatic point of view, one can state that the two houses are located in the same climatic region. The location of the monitoring sites has been presented in Fig. 2.

The first monitored building (Huy) is a semi-detached house of the early 20th century but significant insulation work of walls and roofs has been conducted. Single-glazing windows have been replaced by double-glazing windows and a balanced ventilation has been installed. However, terminal units still consist of high temperature radiators. The family that lives there consists of 2 active adults and 3 children under the age of 10.

The second monitored building (Oostmalle) is a full detached house from the 70s but tremendous renovation just took place before the study. Insulation has been increased of course, but the whole space heating architecture has also been revisited with the implementation of floor heating for the ground floor. On the first floor, terminal units consist of high temperature radiators as in the former house. The family consists of a young active couple with one child of a small age. Compared to the previous house, this dwelling has the particularity of using its floor heating all year long, even in the summer.

Whereas the buildings and occupants utilization are different, both machines can be considered as identical with "by default" parametrization (except for heat demand potential scheduling).

Fig. 2. Location of the monitoring sites.

2.3. The measurement devices and data acquisition

Both houses are equally monitored. Sensors are identical and are placed at the same spots, according to the simplified scheme of Fig. 3. Sensor reference, precision and resolution of the acquired data are presented in Table 2.

Last very important parameter not shown in Table 2 is the sampling rate, the frequency of the acquisition. With this data logger and its "T2" communication mode [22], it is impossible to set a time step smaller than 2 min due to the fact that it must establish a successful Wireless M−bus (Meter-bus) connection with every sensor, one after the other, and that takes time (a few seconds for each connection) [22].

Except for temperatures and humidity, all of those meters are computing energy index values (always increasing). Only the heat meters are also able to provide the instantaneous power but the quite large monitoring sampling time is not sufficient for energy calculations and balances.

The heat meters are basing their energy index on the integration of their flow rate measurement, combined to (in-pipes) temperature probes on both depart and return lines of the machine (separate PT-500 temperature measurements). They are simply following the first thermodynamics principle based on pre-programmed enthalpy calculations (internal correlation with temperature is implemented). Sensor pre-programming thus depends on the heat transfer fluid (which is simple water in both houses). It also depends on the flow meter position (flow or return circuit) as this will impact the flow meter operating temperature, along with the properties of the fluid being measured. Heat meters are preferably placed on the pipe returning to the machine, as the temperature is lower and more stable. The life of the components is thus extended [23] and both sites considered in this study indeed follow this best practice.

Each electrical energy meter measurements the net electrical flow and is continuously computing its integration into two indexes of energy: one for the electrical production/rejection, one for the electrical consumption. This means that the consumption of the system's auxiliaries cannot be seen while the PEMFC is producing electricity. Similarly, only the net electrical production (minus the power consumption of the auxiliaries) is measured.

At last, the hourly values of the High Heating Value (HHV) of the natural gas mix of both sites have been provided for each field-test site for the whole year by the gas provider. This information, whose process is described in an earlier study [26], allows for achieving a better accuracy for the analyses, since no assumption of "gross average" calorific values of the gas mix had to be made.

Maximum relative propagated uncertainty on electrical and thermal efficiency calculations (from sensors described in Table 2) can respectively be considered to be about ± 2% and ± 5% without considering the potential unoptimized placement of sensors (especially for thermal probes). Uncertainty propagation has been conducted according to the National Institute of Standards and Technology method similar to what is described in a parallel study conducted on another fuel cell system [27].

2.4. Black-box modelling instead of component modelling

The whole internal control of the machine has trivially a significant impact on its performance and a theoretical model based on the different components within the system seen in Fig. 1 (a) would unlikely reproduce it with accuracy. Indeed, even though those components are quite simple (heat exchangers, pumps, three-way valves, gas condensing boiler, DHW water tank, fuel cell as a heat and power generator), the way they are combined with each other and the way they are controlled is only known to the OEM.

Furthermore, the OEM's control, affecting the model, is likely to

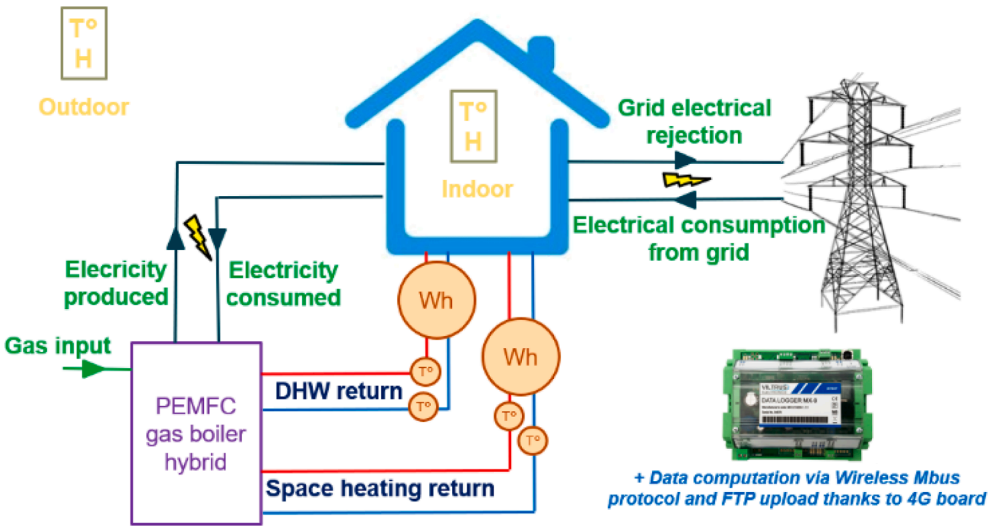

Fig. 3. Monitoring sensors configuration for both houses using the studied PEMFC system.

Table 2
Reference of the monitoring sensors.

Sensors	Reference	Resolution (data logger included)	Accuracy
Outdoor temperature and humidity	Weptech Munia	0,1 K | 0,1 %	± 0,3 K | ± 2 %
Indoor temperature and humidity	Weptech Munia	0,1 K | 0,1 %	± 0,3 K | ± 2 %
DHW and space heating heat counters	Qalcosonic E1 Qn2,5 q_i = 0.025 m^3/h | L = 130 mm	1 kWh | 1 L | 0,1 K	Accuracy Class 2 [24]
Machine and house 2-ways electrical energy counters	Qalcosonic E1 Qn2,5 q_i = 0.025 m^3/h | L = 130 mm	10 Wh	Accuracy Class 1 [25]
Gas volume counter	BK-G4T DN25 Qmax 6 m^3/h	10 L	<0.5%
Data logger (cloud connection)	Viltrus MX-9	NA	NA

consider extra parameters that this study could not collect. For example, in the field-test, one is studying real machines installed in real homes, with real occupants, that can modify some control parameters anytime they want, such as ambient temperature setpoint, heating schedule and heating curve. Also, the machines are usually connected to the internet allowing the OEM to install updates in the control and any component modelling could instantaneously become obsolete.

Therefore, it is preferable to build a performance model ("black-box" model) of the system based on empirical monitoring results that is robust to all those potential changes. The performance model will rely on the measurements of all incoming and outgoing energy flows as shown in Fig. 3.

It is however expected that the variance of the resulting models and their goodness of fit will of course still be affected by potential difference in internal control, usage and parametrization of the system.

On one hand, the main advantage of "black-box" modelling is that it requires limited and simple inputs, such as the building heat demands, easy to establish with common building performance simulation tools. For example, the simplest models developed in this work have been designed to be applicable to any building, being only based upon the heat demand indicator expressed in kWh/m2 indicated in the building's European performance certificate (today mandatory [28]).

On the other hand, the main limitation of "black-box" modelling is that the related states of the internal components of the system are not established. Therefore, the models proposed in this work can hardly help understanding and improving the way those internal components are controlled. This could have been provided thanks to a specific modelling of the internal components, but it would have likely required additional monitoring sensors to be placed between those internal components. Unfortunately, this could not be performed in this case due to occupants' warranty policies. Thus, there was no available measurement between the components so even deducing the control laws of one single component (such as one electrical three-way valve) would come with great uncertainties.

In this case, the described "black-box" modelling method is therefore a more suitable (and practical) option.

2.5. The time bases of the models

Modelling performance based on small timesteps (down to the minute or the second) is not relevant in this case for several reasons.

First, as explained earlier, the monitoring sample time cannot be smaller than 2 min so the chosen modelling timestep must be (significantly) greater. Also, it is only an average sample time: the timeframe between two wireless communications from the sensor to the data logger is not regular as the communication time itself is not regular with the Wireless M−bus protocol.

Second, information from the sensors is provided as energy indexes (with a resolution that is not sufficient for instantaneous calculations) and establishing the derivative of the signals provides too much noise.

Furthermore, it is worth remembering that the sensors are communicating with the data logger one at a time and that the signals are not sufficiently synchronous for analyses on quite small timesteps.

At last, it has been stated that no sensor could be placed inside the systems for warranty reasons and the heat stored in the tank is not monitored.

Therefore, one must analyze the performance of the system over a certain timeframe. It is assumed that the smallest timeframe is 24 h as it corresponds to occupants' natural (daily) cycles (DHW production scheduling, for example). However, even with a 24-hour timeframe, as it will be explained in this section, the effect of the storage tank (that could be heated one day and emptied the next one) can still cause significant dispersion and impede the goodness of fit of the daily models developed in this paper. Therefore, in addition to daily-based models, a monthly-

based model will also be reported in this work. Both time bases will be compared in terms of goodness of fit.

2.6. The modelling primary philosophy and its successive improvements

As stated, this work's primary purpose is to build an empirical "black-box" model that is estimating the daily (or monthly) electrical and thermal efficiency of the PEMFC – gas boiler hybrid system according to daily (or monthly) heat demands (DHW and space heating). As the heat demands can easily be measured, computed or estimated for any building, the primary model can be easily applicable.

The primary established daily-based model will then be enhanced by considering some other influencing factors that will bring increased accuracy and goodness of fit, but that will require extra data, not always available. Therefore, the methods used to enhance the model by considering working temperature and/or the ability of the machine to modulate its heat rate output might be more relevant than the resulting enhanced models themselves for potential other similar studies.

The first improvement will come by considering the working temperature: as expected from literature [5], the higher it is, the lower the thermal efficiency. This means that the system will perform better with low temperature terminal units such as floor heating. This can be explained by the increased ability of the system to condense and recover heat from its flue gases [5] and it applies both to the boiler and the PEMFC of the system.

The second one will come by considering the behavior of the heat demand: highly transient and "ON/OFF" heat demands will lower the thermal efficiency. As for the working temperature influencing factor, this second influencing factor can be partially linked to the terminal units as well. Indeed, for example, floor heating has greater inertia and thus requires longer and smoother heat productions.

At last, the daily-based model is even enhanced by considering as an input the PEMFC load factor, i.e. the achievable daily electrical production, i.e. its achievable operating time. Unfortunately, in reality, daily achievable electrical production is not exactly an "input" such as the two "influencing factors" previously cited and used for enhancing the models. However, the system is not electrically driven and is supposed to provide electricity as constantly as possible (which is desired for durability reasons [29]). Therefore, the PEMFC load factor is thus a consequence of the ability of the fuel cell to stay "ON" and it depends on external factors, such as the thermal management of the fuel cell. Indeed, the PEMFC stops if it is no longer able to dissipate its heat either in the tank or in the space heating. In fact, PEMFC thermal management is key to ensure its lifetime as literature reports that PEMFC could be stopped for improper thermal conditions (to ensure its integrity [29]) and this is probably why the OEM states the maximum internal return temperature to the fuel cell reaches 50 °C [30]. Unfortunately, that condition is very difficult to identify based on the collected data as it has been explained that the monitoring campaign could not include sensors inside the machine (and especially on the storage tank).

Since thermal conditions around the PEMFC are critical regarding the ability of the fuel cell to operate for long duration, the fuel cell load factor will depend the amount of heat that can be stored by the fuel cell in the storage tank (considering heat withdrawals including those that accounts for DHW) and/or the amount of heat that can be delivered to the space heating. In fact, this latter is partially dependent on the two previously cited influencing factors used to enhance the primary model (working temperature and heat demand behavior).

Thus, instead of considering the PEMFC load factor as a model input, further work might allow its modelling as a function of tangible influencing and predictable factors such as the heat demands of the building and occupants, their absolute daily values, their smoothness over the day, their average working temperature, *etc*….

In the meantime, for this paper, the PEMFC load factor is taken into account for this modelling as an input as is. This input shall be considered as a daily indication of the adequation of the system (and its control) with the installation and with its occupants.

It should be noted that the load factor is usually defined as the current power level relative to the maximum [31]. In this case, since the PEMFC is either turned "OFF" or "ON" at its nominal power, it is more relevant to use the load factor on a daily (energy) basis, i.e. the total daily electrical production divided by the maximum it could have produced (which is equal to 18 kWh_{el}, considering a nominal output power of 0.75 kW_{el} for 24 h).

3. Modelling

3.1. Key parameters – Electrical and thermal efficiencies both depend on heat demands

The most important contribution to such a "black-box" model is to find key parameters on which the whole performance indicators can be deduced despite the specific parametrization, use and control.

Thanks to Fig. 1 (b), one can consider the electrical efficiency of the fuel cell only as constant. However, for the same duration of fuel cell utilization, the burner might not provide the same heating capacity: it can be shut down completely the whole day as well as it can be providing heat at nominal output rate. Therefore, the daily (or monthly) electrical efficiency will be affected by the heat production (and the way it is produced).

Furthermore, the gas boiler heat production has not only a direct impact on the electrical efficiency but it has also an indirect impact: indeed, the elevation of the return temperature due to the gas condensing boiler being turned "ON" for space heating (especially with high temperature terminal units) could prevent the fuel cell from dissipating enough of its heat and force its temporarily shut down.

Fig. 1 (b) also shows that thermal efficiency of the running fuel cell only cannot be assumed constant and depend on the working temperature conditions, which are themselves particularly affected by the heat demands of the house and the state of possible other heating appliances. For example, if the gas condensing boiler has to be turned "ON" to meet the heat demand, it will likely elevate the return temperature to the fuel cell and decrease the efficiency of the heat transfer.

Thus, both the electrical and thermal daily efficiencies depend on the

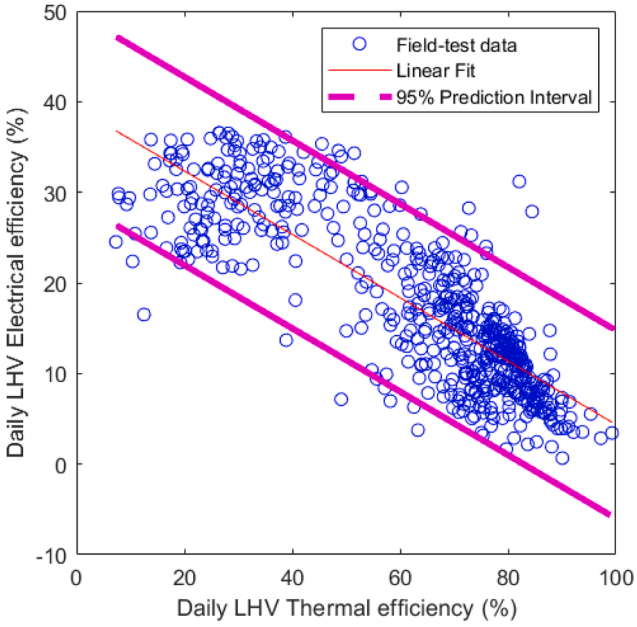

Fig. 4. Linear fit of the field-test daily electrical efficiency according to the daily thermal efficiency. The 95% confidence interval is however quite large as it defines a ± 10 percentage points zone around the fit for the daily electrical efficiency.

heat demands of the house and one can even link them together. Indeed, there is even a gross linear trend between the daily thermal and electrical efficiencies, as shown on Fig. 4.

Based on Fig. 4, a linear relation between LHV daily electrical efficiency η_{el} and LHV daily thermal efficiency η_{th} can be defined by Equation (1):

$$\eta_{el}(\%) = 39.34 - 0.35\eta_{th} \quad (1)$$

As a first approach, with Equation (1), one can therefore establish that modelling only the daily thermal efficiency of the unit would suffice to model the whole system daily performance. It should be considered that Equation (1) is not valid for low LHV thermal efficiencies (under about 10%) because electrical LHV efficiency of the PEMFC only cannot be higher than 37% (Table 1). A very similar linear relation to Equation (1), with coefficients (and confidence intervals) almost identical, can also be established between electrical and thermal efficiency on a monthly-basis instead of on a daily-basis.

It should be noted that the electrical consumption of the system (that is measured when the fuel cell is not running) is neglected in the efficiency calculations. The denominators of the established efficiencies consist only of the consumed gas expressed in LHV (thanks to a HHV to LHV assumed ratio of 1.1085 [14]).

3.2. Simple single-variable time-invariant thermal efficiency models

Literature on monitoring gas condensing boilers combined with DHW storage tanks [32] has studied the relation between monthly LHV thermal efficiency and heat demand. The results show that a clear logarithmic trend can be deduced with an asymptotic limit as heat demand increases.

The same kind of results has been computed for the two systems of this work both on a daily and a monthly-basis. Also, based on those results, logarithmic simple model relations have been optimized automatically thanks to the Matlab software. The logarithmic models have as general equation the relation dictated by Equation (2), where η_{th} is the daily (or monthly) thermal LHV efficiency (expressed in %), Q_{SH} and Q_{DHW} are respectively the daily (or monthly) space heating demand and the DHW demand (expressed in kWh) and C_1, C_2, C_3 are the constants that have been set automatically to optimize goodness of fit compared to empirical results (values given in Table 3).

$$\eta_{th}(\%) = C_1 + C_2 log[(Q_{SH} + Q_{DHW}) + C_3] \quad (2)$$

Graphical results and coefficients of the monthly model based on Equation (2) are respectively reported in Fig. 5 and Table 3. Goodness of fit can be studied easily with the Matlab software as RMSE and R-square values (chosen indicators for this study) have been established in Table 3. The following explanations have been provided by the Matlab Software support [33]:

- R-square: This statistic measures how successful the fit is in explaining the variation of the data. Put another way, R-square is the square of the correlation between the response values and the predicted response values. R-square can take on any value between 0 and 1, with a value closer to 1 indicating that a greater proportion of variance is accounted for by the model;
- RMSE: This statistic is also known as the fit standard error and the standard error of the regression. It is an estimate of the standard deviation of the random component in the data. RMSE value closer to 0 indicates a fit that is more useful for prediction.

Table 3
Values for the parameters of the logarithmic models and goodness of fit indicators.

Parameters & fit results	Monthly model ($_m$)	First daily model ($_d$)	Second daily model ($'_d$)	Third daily model ($''_d$)
$C_{1m}\|C_{1d}\|C'_{1d}\|C''_{1d}$	−127.9	3.491	−2.035	−0.06732
$C_{2m}\|C_{2d}\|C'_{2d}\|C''_{2d}$	14.1	17.59	19.93	19.1
$C_{3m}\|C_{3d}\|C'_{3d}\|C''_{3d}$	$-3.3e^{-4}$	0.7636	1.13	0.9973
R-Square	0.9721	0.8974	0.8984	0.8937
RMSE	3.6020	7.9003	7.8621	7.8225

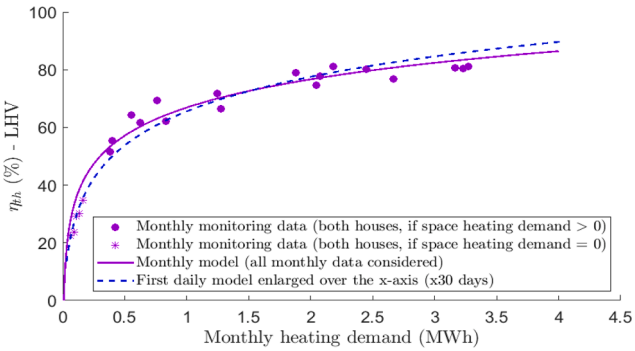

Fig. 5. Comparison between the monthly and the first daily model defined by Equation (2) and whose coefficients are given in Table 3. To allow the comparison, the daily heat demand from the first daily model has been multiplied by the average number of days contained within a month, i.e. 30. As stated in Section 2.2 - *The monitored houses*, in the summer, the house in Huy has completely shut down its space heating and its system was only used for DHW. These monthly data were separated from the others monthly data to show that the models are relevant no matter if the system is used for DHW only or also for space heating.

Graphical results of the daily model based on Equation (2) are reported at the top of Fig. 6. Again, Table 3 reports the coefficients from Equation (2) but also its goodness of fit indicators.

In this case, after removing some inconsistent data mainly originated from monitoring signals losses (only for the daily models), R-square values for all of the single-variable daily models proposed in this work are always close to 89.5%, meaning that even the simplest model explains already about 90% of the total variation in the data about the average, which is quite significant already. In fact, the further single-variable daily models do not improve the R-square value.

Thus, the goodness of fit of the first daily model is sufficient whereas it is extremely satisfying with the monthly model. In fact, the difference in the goodness of fit indicators between the monthly and the (first) daily model(s) can mostly be explained by the effect of the internal DHW storage tank that causes significant dispersions on the daily performance. Indeed, as mentioned in *Section 2.5 - The time bases of the models*, with daily timeframes, the DWH tank could be heated one day (worsening the thermal efficiency of that day) and emptied the next one (improving the thermal efficiency of that following day.

For example, based on the tank capacity of 220 L of water that is considered as empty with an average temperature of 30 °C and loaded with an average temperature of 60 °C, the total energy considered to be stored is 7.67 kWh. Knowing that the average observed daily DHW consumption of both systems in the whole year 2020 is about 5 kWh, one can in fact imagine the “worst case” impact that the storage could have on the variance of the thermal efficiency, especially in summer where space heating is null or minimum. However, DHW production is usually scheduled daily in those systems (with a function called “DHW priority”) [34], as standby heat losses prevent the temperature to stay sufficiently high to ensure DHW for the following day (even if there were no DHW consumption).

Comfort is not the only requirement to regularly keep the temperature of the tank quite high as Legionella prevention also advises it [35]. Therefore, DHW production variance fortunately does not reach the “worst case” stated here above and only an uncertain smaller proportion of the tank is actually used on the following day rather than on the actual

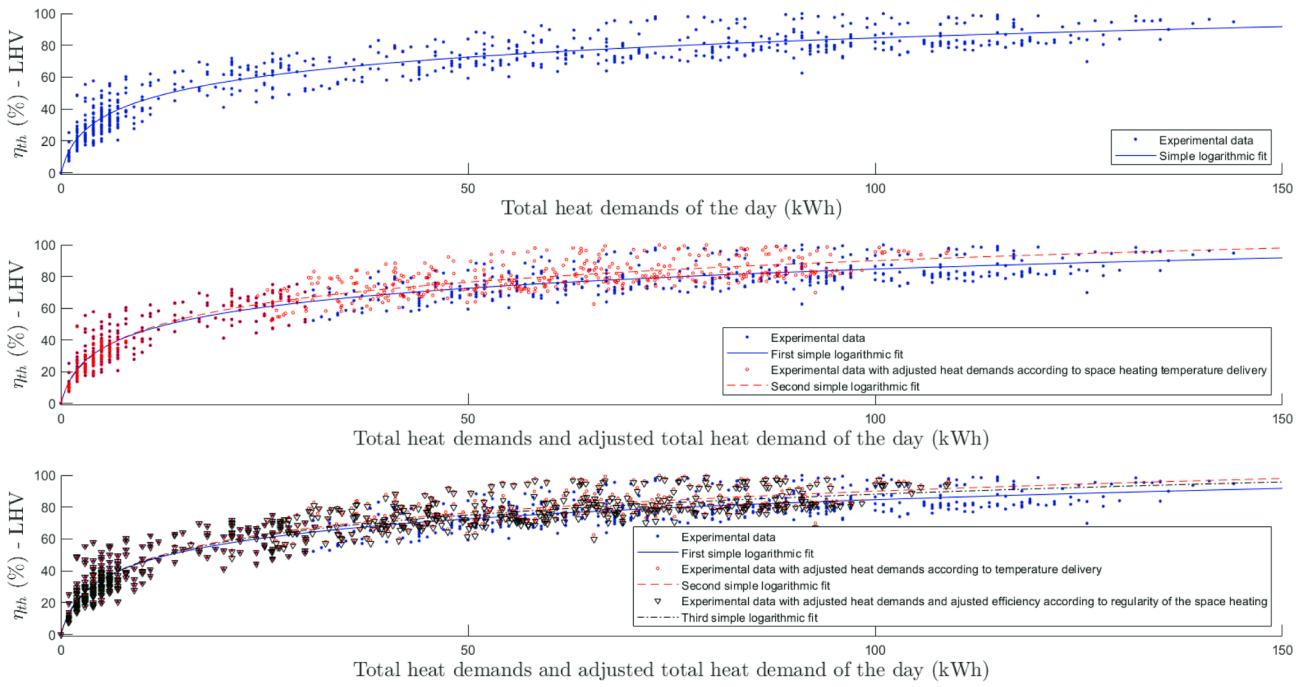

Fig. 6. Step by step improvement of the primary logarithmic empirical model defined by Equation (2) to account for key effects on thermal efficiency.

day. Still, this reflects on the R-square value of the single-variable daily models as this work considers the machine as a whole (gas condensing boiler + fuel cell + storage tank) without modelling the storage effect individually. Unfortunately, as it has already been stated, one could not monitor the state of the internal tank by lack of internal sensors (for warranty reasons).

It would be expected that the kind of daily dispersion caused by the DHW storage tank leads to a distribution of residuals that is spread quite equivalently around the prediction of the daily model. This is actually confirmed by the fact that Fig. 5 indicates that, on the same time base, the daily model is validated by its similarity with the monthly model (that shows amazing goodness of fit indicators). Therefore, both models can be considered as quite equivalent and relevant for the application (despite the daily dispersion of the performance due to the DHW tank).

Still, it is possible to improve the single-variable daily model by considering other sources of performance dispersion occurring with the field-test systems. Unfortunately, the intrinsic errors due to the accuracy of the sensors (Table 2) unfortunately cannot be easily compensated in the models. However, the performance of space heating appliances are generally still affected by their operating temperature [5] and their dynamic behavior [6] regarding the heat demands profiles, which can be quite erratic or stable. Those effects are not considered in the first daily model and, as it will be seen in the following section, this is the purpose of the second and third daily models.

It is worth mentioning that only the two-variable daily models in the next section will also allow significantly better goodness of fit indicators compared to the single-variable daily models.

3.3. Improved daily thermal efficiency models

3.3.1. Operating temperature

Literature on gas condensing boilers has stated that operating temperature (mainly return temperature for condensation reasons) can have a significant effect on thermal efficiency, even outside the ensured condensing mode zone (because of increased ambient losses) [5]. Also, for the PEMFC, the OEM has also reported in Fig. 1 (b) a thermal efficiency decrease with increased operating temperatures. Therefore, one might improve the first model by taking into account the working temperature of the machine (by considering the return temperature). There are several ways to account for this but one shall look at the return line temperature (inlet line for the machine), as it is done in literature [5]. In this case, one shall also preferably look at the space heating circuit for four main reasons:

- DHW can be assumed to be delivered at approximately the same temperature (for comfort and Legionella reasons [34]). Plus, inlet sanitary water comes from the water mains and will also be measured at approximately the same temperature (ambient or slightly lower).
- DHW daily production (with the boiler) is usually short in time and is represented by highly transient operating conditions. This would thus be very hard to distinguish the performance decrease due to the transient effects and the one due to the temperature levels.
- In this case, DHW production mainly goes into the storage tank and is not measured by the monitoring sensors.
- At last, over the whole monitored year, space heating use is far more prevalent than DHW production. For example, for the house in Huy, annual space heating demand is 12.5 times higher than DHW demand and this ratio goes up to 16.5 for the house in Oostmalle.

Since one is studying daily efficiency figures, it is wanted to build one single daily indicator that will represent the working temperature of the whole day. The problem is that the machine does not work in steady-state operations for the whole day. Looking only at the maximum temperature of the day in the return line would therefore not be representative of the whole day and might account for one single (very high) transient effect. Looking at the average temperature of the whole day is not ideal as well because a very erratic and high temperature space heating demand could result in the same average temperature as the one of a 24-hour long low temperature demand (typical of floor heating).

Therefore, it has been chosen in this work to look at the 4-hour gliding average of the return temperature and keep its maximum value of the day $\overline{T_{R,4h}}$.

The correction factor γ_1 for space heating working temperature is applied on the horizontal axis (total heat demands: $Q_{SH} + Q_{DHW}$) by adjusting the heat demands according to Equation (3).

$$(Q_{SH} + Q_{DHW})_{aj} = (Q_{SH} + Q_{DHW}) * \gamma_1 \quad (3)$$

This operation is presented in a flowchart in Fig. 7 which also shows the impact of this correction factor on the generic logarithmic equation of the model defined by Equation (2).

For low heat demands (warmer seasons), this adjustment shall not be applied as the system is mainly (and sometimes only) used for DHW and not for space heating. In this work, the limit to apply the correction factor has been set manually (to minimize RMSE) to 30 kWh. Although space heating is usually always seen with total heat demands over 10 kWh, the rather high proportion of the DHW demand in the 0–30 kWh total heat demands window prevents the fit to be improved that way. Over the 30-kWh limit, the DHW part in the total heat demands becomes sufficiently low for the correction factor to be applied. In this applicable window, the relation between thermal efficiency of the day and total heat demands has been considered as linear (see the top of Fig. 6). As a first approach, for the same total heat demands, the relation between thermal efficiency and the maximum 4-hour gliding average temperature of the day on the return line $\overline{T_{R,4h}}$ can also be considered as linear.

In fact, as it can be seen in Fig. 8 (a), higher the total heat demand, higher the decrease in efficiency according to operating temperatures (maximum 4-hour gliding average temperature of the day on the return line). This validates the application of γ_1 in Equation (3) as a correction factor applied relative to the total heat demand of the day. γ_1 is defined according to Equation (4), $\overline{T_{R,4h}}$ having been explained here above and $Max_{\overline{T_{R,4h}}}$ being the maximum value of the daily $\overline{T_{R,4h}}$ values of the dataset for the whole studied year (nondimensionalization):

$$\gamma_1 = 1 - \frac{\overline{T_{R,4h}}}{Max_{\overline{T_{R,4h}}}} * 0.3 \quad (4)$$

This data manipulation results in updated constants for the generic logarithmic model described by Equation (2) as well as small improvements of the RMSE and the R-Square value, as it can be deduced from Table 3. The resulting fit is presented in the middle graph of Fig. 6. The weight of the correction implied by γ_1 in Equation (4), i.e. the 0.3 value, has been optimized manually.

3.3.2. *Transient effects & power peaks*

As it is generally the case in engineering, it is better to operate a machine in steady-state conditions or as close as possible to those. In fact, one purpose of the storage tank of this system is indeed the increased thermal inertia it allows in order to smooth up the behavior as much as possible. Although, paradoxically, the tank accumulates heat and therefore intrinsically impedes steady-state conditions.

However, even with the tank, oversized space heating appliances and/or erratic demand set by the user can cause highly dynamic behaviors that induce decreased efficiencies.

This is also true with gas condensing boilers as it has been found in literature that improving their level of modulation, increasing the duration for which the machine operates in steady state conditions, can lead to an improved efficiency of about 4 percentage points [6].

This effect has also been studied in this work and integrated into the

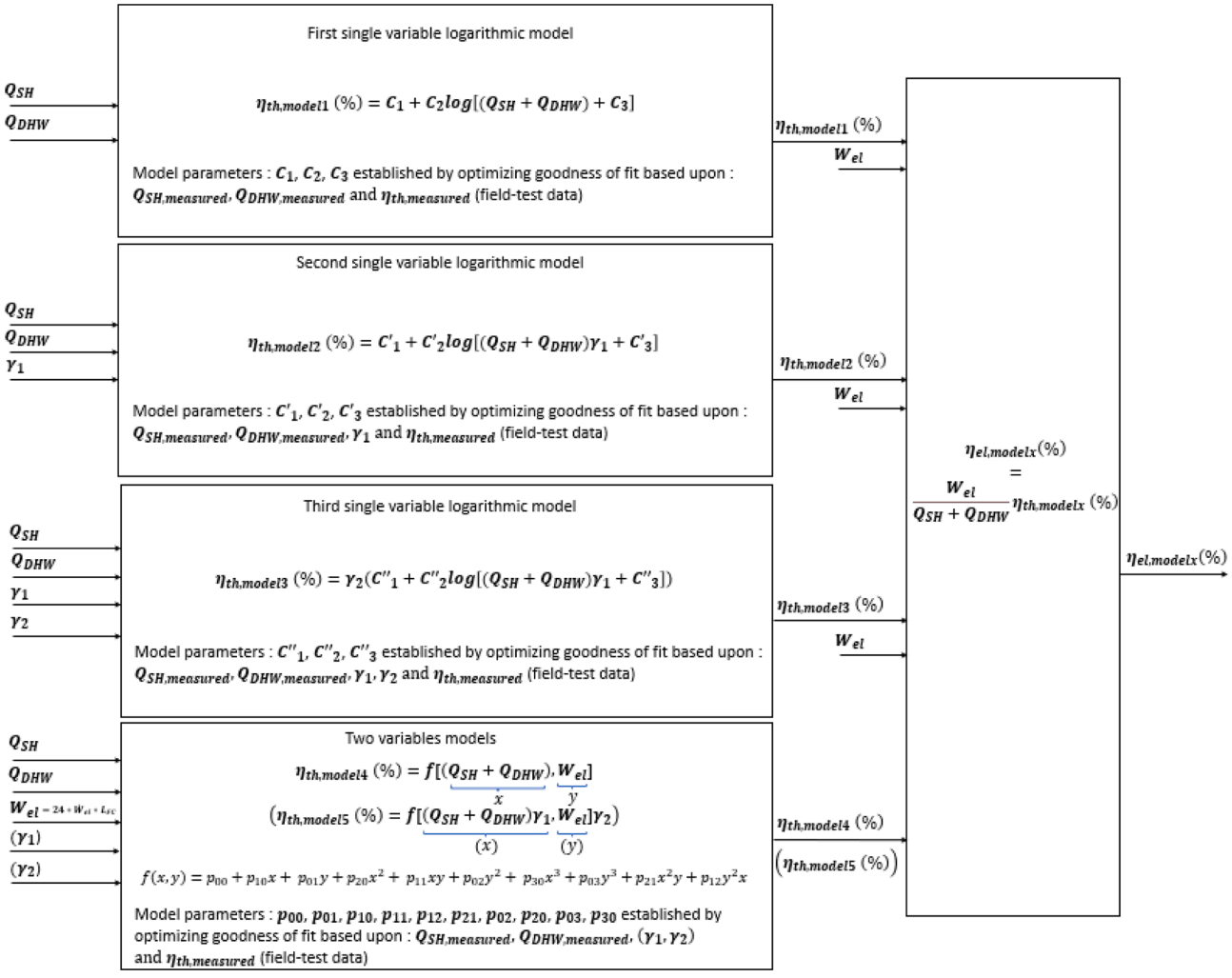

Fig. 7. Flowchart of the daily models developed in this field-test study.

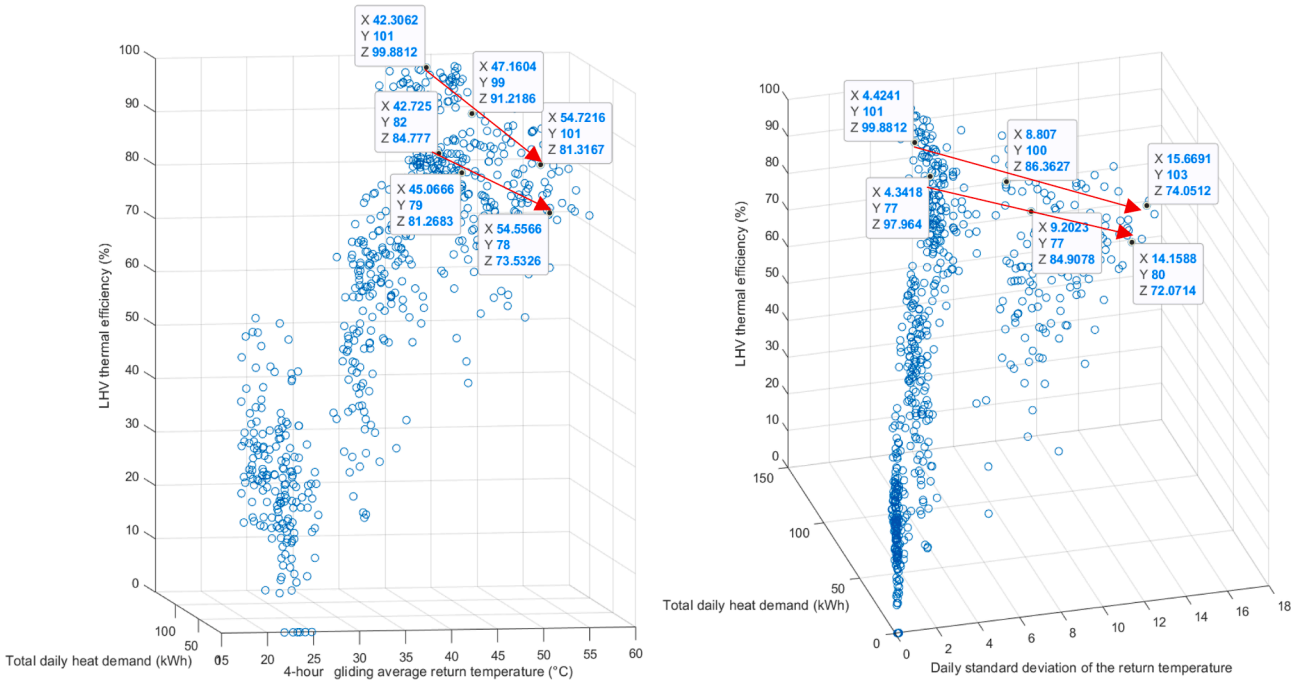

(a) (b)

Fig. 8. (a) Small decrease (considered linear) of thermal efficiency according to the operating temperature for identical total heat demands; **(b)** Small decrease (considered linear) of thermal efficiency according to the standard deviation of the return temperature for identical total heat demands. Six days have been highlighted per graph: X is either the 4-hour gliding average temperature or the daily standard deviation of the return temperature, Y is the total daily heat demand and Z is the LHV thermal efficiency.

single-variable logarithmic model with a similar method as the "working temperature effect" conducted in the previous section. This is done by establishing a second correction factor γ_2 as described by Equation (5) that is directly applied to the daily thermal efficiency (that becomes the adjusted daily thermal efficiency $\eta_{th_{aj}}$).

$$\eta_{th_{aj}}(\%) = \eta_{th}{}^{*}\gamma_2 \tag{5}$$

Again, this operation is presented in a flowchart in Fig. 7 which also shows the impact of this correction factor on the generic logarithmic equation of the model.

To account for the effect of the erratic space heating demand and establish γ_2, it has been chosen again to observe the space heating return temperature and compute its standard deviation over the whole day (σ_{TR}), which effect on the thermal efficiency is presented in Fig. 8 (b). Again, it has been chosen not to affect the correction factor γ_2 on the whole dataset. Indeed, smaller standard deviations in warmer seasons (with low or null space heating) can be explained mainly by the fact that the variance in the efficiency results comes mainly from the storage tank not modelled in this work, as explained earlier.

In addition, since standard deviation of the ambient temperature, where the sensor is placed, can also account for part of the standard deviation of the return temperature, it has been chosen to limit the application of the second correction factor γ_2 on the daily data that have standard deviation above 3.25. Therefore, there is no need to set another application window on the total heat demands figures as it has been done in the previous method.

Thus, γ_2 is established by Equation (6), σ_{TR} having been explained here above and $Max_{\sigma_{TR}}$ being the maximum value of the daily σ_{TR} values of the dataset of the whole studied year (nondimensionalization):

$$\gamma_2 = 1 - \frac{\sigma_{TR}}{Max_{\sigma_{TR}}}{}^{*}0.05 \tag{6}$$

However, there is a significant difference with the "working temperature" correction method established in the previous section: it is visible in the lower part of Fig. 6 that the correction factor is applied on the vertical axis this time. It is indeed applied directly on the thermal efficiency as induced by Equation (5).

The γ_2 correction factor means that erratic behavior of the machine can lead up to a 5% decrease in efficiency (based on data already adjusted by the previous method to account for working temperatures). This has been optimized manually and is relevant with consulted literature as it is close to the 4-percentage points decrease cited earlier [6].

This second correction leads to the third and last of the single-variable models presented in this paper, shown in the bottom of Fig. 6 and whose goodness of fit is established in Table 3.

3.3.3. *Two-variables models*

The fact that the PEMFC has intrinsically a worsen thermal efficiency than the boiler, as seen in Table 1, implies that the PEMFC daily electrical production affects the daily thermal efficiency of the system.

This comes in addition to the fact that most of the heat from the fuel cell goes in the tank and is thus subject to standby losses. Indeed, in winter, the heat demand is too high and the boiler needs to provide thermal energy directly to the hydraulically circuits of the house and in summer, mainly DHW from the tank is needed.

Up till now, the single-variable models developed in this paper that fitted the data sufficiently already have not considered this effect, particularly significant in warmer seasons. This can be studied further by extending the models with an additional dimension, simply being the PEMFC daily load factor L_{FC} (defined earlier as the daily electrical production over the maximum value it can reach, i.e. 18 kWh_{el}). The resulting two-variables models have been plotted in Fig. 9.

The first model considers the adjusted data from the last single-variable model developed in the previous section to account for the working temperature effect as well as the smoothness of the modulation of thermal energy. The second model is not considering those effects and

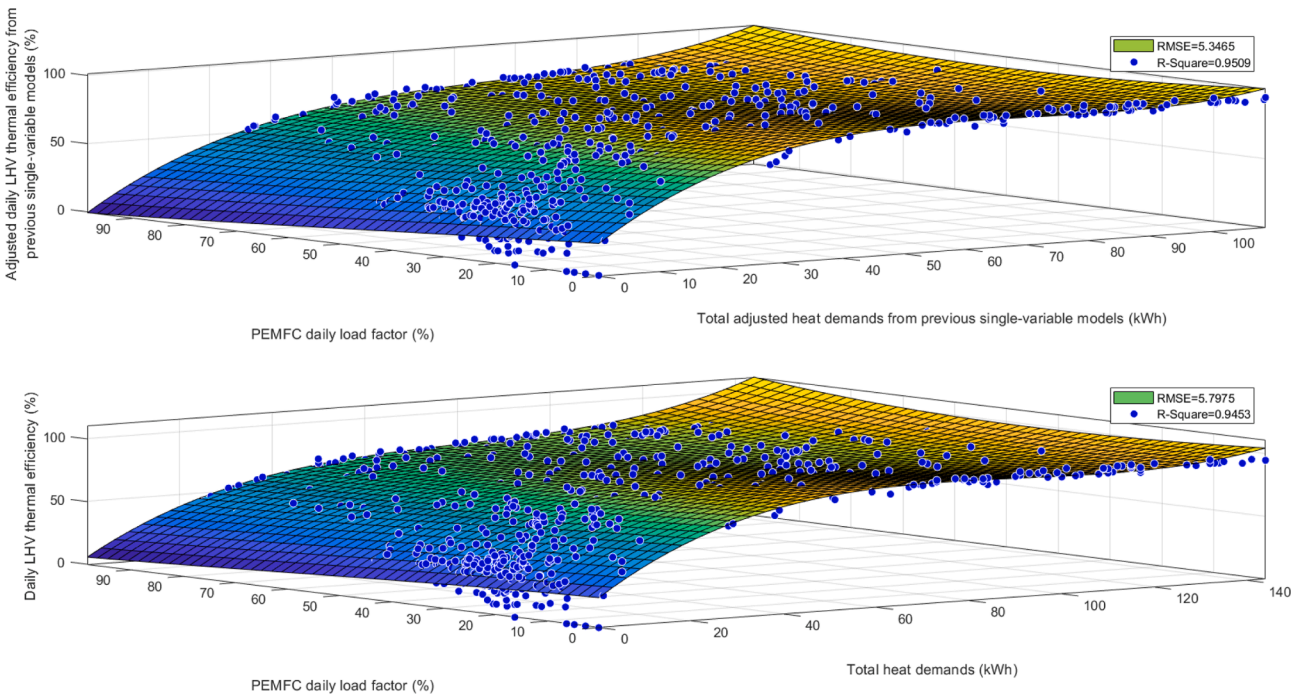

Fig. 9. Final two-variable models of this work. The first one includes the corrections made in the previous single-variable models (according to working temperatures and modulation smoothness) and provides a better fit. The data of the second one has not been postprocessed.

it provides a sufficient but slightly worsen goodness of fit.

For both two-variable models, one can directly see a significantly better goodness of fit compared to previous single-variable models (even with R-square values). Both models are polynomial regressions of the third order on both dimensions performed thanks to the *Matlab* software with robust least squares fitting option called "bisquare", which consists of minimizing a weighted sum of squares, where the weight given to each data point depends on how far the point is from the fitted curve. The resulting models are defined by Equation (7) (x being the total heat demands or the adjusted total heat demands and y being the daily electrical production deduced from the PEMFC load factor and its nominal electrical output power).

$$f(x,y) = p_{00} + p_{10}x + p_{01}y + p_{20}x^2 + p_{11}xy + p_{02}y^2 + p_{30}x^3 + p_{03}y^3 + p_{21}x^2y + p_{12}y^2x \quad (7)$$

The values of the constants for both models are given in Table 4.

Main remaining errors of both models come again from very low total heat demands, again due to the prevalent effect of the storage tank. As explained, the tank can deliver thermal energy stored the day before and causes great variance in the results, which is visible on the bottom part of each graph of Fig. 9). Part of the remaining error can also come from the potential difference in parametrization of the system by the installer or the user and from the intrinsic uncertainties due the accuracy range of the sensors reported in Table 2.

These models have also been presented in the flowchart of Fig. 7.

It shall be mentioned that the two-variables model defined by Equation (7) and which coefficients are given in the first row of Table 4 has been compared to steady-state laboratory experiments on the same CHP system [3] and correlation could be demonstrated [36].

3.4. Electrical efficiency

In this work, the priority has been put on the thermal efficiency for several reasons:

- It is the main contributor of the total efficiency as it can be deduced from Fig. 1 (b) or Fig. 4.
- As a first approach, there is a simple linear trend between thermal and electrical efficiency, as shown in Fig. 4, and Equation (1) can easily be used to estimate it.

If one wants to go further than this not very accurate linear trend and if the PEMFC daily load factor L_{FC} is known (which should be the case for the two-variables models to be implemented), the daily electrical efficiency η_{el} could be calculated with Equation (8):

$$\eta_{el} = \frac{W_{el}}{Q_{g,LHV}} = \frac{L_{FC}*24*\dot{W}_{el}}{Q_{g,LHV}} \quad (8)$$

Where W_{el} is the daily electrical production calculated based on $\dot{W}_{el}$, the nominal PEMFC output electrical power (0.75 kW_{el} in this case). $Q_{g,LHV}$ has been linked to the thermal efficiency in Equation (9) and corresponds to the LHV content of the gas consumed by the machine on the day. It could be grossly considered equal to the volume of gas consumed times the LHV figure established by the gas provider. However, it has been demonstrated in an earlier study that it is more accurate to implement a correction factor to the monitored gas volume to account for the pressure and temperature measurement difference between the measuring conditions (in the gas pipe upstream the system) and the standard conditions at which the LHV are defined by the gas provider [26].

Table 4
Values for the parameters of the two-variables models with and without adjusted data.

Models	p_{00}	p_{01}	p_{10}	p_{02}	p_{11}	p_{20}	p_{03}	p_{12}	p_{21}	p_{30}
1. with adjusted data	24.27	−1.648	3.024	0.01102	−0.01704	−0.04291	7.329e-5	6.384e-4	1.597e-4	1.976e-4
2. without adjusted data	24.76	−0.9458	2.494	−0.01896	−0.02719	−0.02819	5.325e-4	7.05e-4	1.642e-4	1.02e-4

$$Q_{g,LHV} = \frac{Q_{SH} + Q_{DHW}}{\eta_{th}} \quad (9)$$

Q_{SH}, Q_{DHW} and η_{th} have already been explained earlier and are either inputs or outputs of the models established in this work.

So, one obtains Equation (10):

$$\eta_{el}(\%) = \frac{L_{FC}{}^{*}24^{*}\dot{W}_{el}}{Q_{SH} + Q_{DHW}}\,\eta_{th} \quad (10)$$

This can even be detailed thanks to the equation of η_{th} given by the single-variable models of this work. For example, the use of Equation (2) relative to the first and most simple daily model developed in this work leads to (C_{1d}, C_{2d}, C_{3d} values given in Table 3):

$$\eta_{el} = \frac{W_{el}}{Q_{SH} + Q_{DHW}}\left(C_1 + C_2 log[(Q_{SH} + Q_{DHW}) + C_3]\right) \quad (11)$$

The other models of this work that provide η_{th} could also similarly be used. However, with the single-variable monthly model (see *Section 3.2 - Simple single-variable time-invariant thermal* efficiency models), it is important to consider in Equation (9) and Equation (11) the monthly load factor of the fuel cell instead of its daily load factor, in addition to replace the 24 coefficient by 720 (=24 × 30).

4. Discussions, limitations & further work

As it can be seen in Fig. 9, the exhibited monitoring PEMFC load factor is often quite low and rarely approaches the ideal 100% target (which would maximize the electrical production of the systems and therefore the cost savings [30]). In fact, the demonstrated PEMFC yearly load factor is always below 50% for both monitored dwellings [30]. Therefore, it could be considered that the high complexity of the hybridization between the PEMFC and the gas boiler (Fig. 1) might not be as optimal in real applications as if those same systems were completely decoupled (with their own standalone separate implementation and control). Indeed, for example, in case of sudden high-temperature demands, the gas boiler must be turned on, which might lead to return temperatures to the PEMFC higher than 50 °C, which have been stated to cause its safety shutdown [30]. In addition, it cannot be excluded from the system's configuration detailed in Fig. 1 that the PEMFC might preheat the return flow to the boiler in some hydraulic configurations (thus lowering its performance and maybe preventing the condensation of the flue gases [5]).

The fact that one might have been studying unoptimized controlled machines and/or unoptimized installations may constitute a limitation to the results of this study but it can in fact be considered that it is the whole point of the monitoring study to take into account those potential unoptimized real conditions in the performance review rather than study controllable optimized laboratory conditions.

Main drawback though is that one may argue that the number of tested machines in this study is far from being enough to statistically be representative. However, obtaining such qualitative correlations between the two machines although the houses they are placed into hold that much difference tend to indicate that the data might in fact be sufficiently representative. In fact, this is also an indication that the installation and the utilization of the machine is consistent with one another.

Nevertheless, caution should be exercised when applying the models developed in this study to very different climatic zones and/or space heating hydraulic configurations.

By design, mainly for durability reasons [29], the heat storage allows the PEMFC to run as long as possible with its small output power. Indeed, it can be assumed that the gas boiler provides heat directly to the outputs (supposably only, when necessary, for very high sudden DHW demand and for space heating), without much heat going through the tank and being subjected to standby losses. Therefore, another key variable not yet studied directly here is the effect caused by the proportion of DHW in the total heat demand of the day. Indeed, as explained, the tank acts as an energy storage, subjected to non negligeable standby losses proportional to the duration of which all the heat will remain in the tank, before finally being measured by the sensors as the house draws DHW.

However, this effect of higher DHW part in the heat demands is already partially considered in the two-variables final models of this work since DHW prevalence in the total daily heat demand occurs in warmer seasons and coincides with lower PEMFC load factor (induced by the fact that the PEMFC is less often able to dissipate its heat in the space heating). Also, Fig. 5 has indicated that the first single-variable models developed in this work (and by extension, their improvement) relevantly predict the system no matter if it produces only DHW or both DHW and space heating. Therefore, the possible improvement of considering the proportion of DHW in the total heat demand of the day/month is not expected to be significant.

Nevertheless, it is assumed that the one evident way to further improve the models would be by considering the internal tank (and its thermal state which would request DHW consumption modelling as well). This would indeed account for a lot of the variance in the data, especially for low total heat demands and daily time bases, as a higher part of the heat stored one day can be released the day after, greatly affecting thermal efficiency. Since it is not possible to place sensors inside the system, a state observer model for the tank might seem relevant. It should be noted that Fig. 5 has indicated that the distribution of residuals due variance of the daily thermal efficiency data due the DHW storage tank is spread quite equivalently around the prediction of the daily model (see *Section 3.2 - Simple single-variable time-invariant thermal* efficiency models). In other words, although a state observer model of the tank will enhance the goodness of fit indicators of the daily models, it would most likely not improve the monthly performance model developed in this work.

At last, the probable best improvement that could be performed to enhance the daily models of this work would be by modelling the PEMFC daily load factor L_{FC} by considering tangible influencing and predictable factors such as the heat demands of the building, their absolute daily values, their smoothness over the day, their average working temperature, the need for fuel cell mandatory regeneration phase [12], etc… Indeed, for the moment, the load factor is used as an input in the best daily thermal efficiency models developed in this work (the two-variable daily models) or is simply used to establish the electrical efficiency accurately thanks to any thermal efficiency model of this work. It is in fact considered as an input indicating the ability of the PEMFC to produce electricity and is therefore an indicator of the adequation between the system, the building and the occupants.

5. Conclusions

This work has developed simple single-variable logarithmic and two-variable regression daily performance models for a PEMFC-gas condensing boiler hybrid system. A monthly single-variable logarithmic performance model has also been established.

As a first approach, electrical efficiency has been assumed to be linearly inversely proportional to the thermal efficiency so the whole system efficiencies could be modelled simply by modelling the thermal efficiency.

All the models of this work require the total daily (or monthly) heat demand of the house, which is the addition of DHW and space heating demands. This is even the single required input for the first simple logarithmic (daily and monthly) models developed in this study, which are defined thanks to Equation (2) and Table 3. This therefore facilitates the applicability of those models since space heating demands can be easily approximated with any building performance simulation and DHW load profiles may be assessed by well-known standards [37].

For example, the applicability of the interpolation models developed in this work can be extended to every homeowner that has an energy

performance certificate as it is mandatory in Europe for any building or building unit which is constructed, sold or rented out to a new tenant [28]. Indeed, those usually involve energy performance indicators expressed in kWh/m^2 per year that could directly help to compute the heat demands used in this work.

This modelling work will thus help evaluating economical and environmental interests of that system in the much-needed energy transition towards a cleaner future.

The monthly performance model exhibits a tremendous goodness of fit. Regarding the daily models, their goodness of fit is inevitably affected by the variance due to the storage effect of the DHW, that can be heated one day and emptied the next one. However, all the daily models of this work still provide sufficient goodness of fit. In fact, the best daily model has been established considering both an adjusted daily total heat demand of the house (adjusted data to account for efficiency decreases related to unoptimized use of the system) and the daily PEMFC load factor (which in this case, must be established).

The adjusted data to compute the best daily model of this work considers two correction factors (γ_1 and γ_2), inspired by gas condensing boiler literature. The first one accounts for the decrease of thermal efficiency related to increased working temperatures. This first correction factor has been established by computing the maximum 4-hour gliding average space heating temperature of each day. The second one accounts for the decrease of efficiency related to unsmooth heat demands. This second correction factor has been established by computing the daily standard variation of the space return temperature.

Eventually, the applicability of the daily models of this work based on the correction factors (γ_1 and γ_2) might be considered as limited to this particular study (and to its corresponding monitoring configuration). However, the methods used to improve them by accounting for nonoptimal uses of domestic heating appliances can easily be reproduced by implementing similar correction factors. Those methods might even be effective with other potential nonoptimal uses of heating systems than the ones reported in this paper, which only considers the impact of operating temperatures and the ability of the system to modulate its heating capacity.

At last, through the quite low PEMFC load factors demonstrated in the field-test monitoring study (reported in Fig. 9), this paper has inferred that the PEMFC and the boiler have been hybridized to such a high and complex level that it prevents both systems to operate as optimally as they would have in standalone decoupled configurations.

Funding: This work was conducted with the partial financial support of Gas.be without any involvement in study design; in the collection, analysis and interpretation of data; in the writing of the report; and in the decision to submit the article for publication.

CRediT authorship contribution statement

Nicolas Paulus: Conceptualization, Formal analysis, Investigation, Resources, Data curation, Writing – original draft, Writing – review & editing, Visualization. **Vincent Lemort:** Writing – review & editing, Supervision, Project administration.

Declaration of Competing Interest

The authors declare that they have no known competing financial interests or personal relationships that could have appeared to influence the work reported in this paper.

Data availability

The data that has been used is confidential.

Appendix A. Supplementary material

Supplementary data to this article can be found online at https://doi.org/10.1016/j.enconman.2023.117634

References

[1] Paulus N. Confronting Nationally Determined Contributions (NDCs) to IPPC's + 2°C carbon budgets through the analyses of France and Wallonia climate policies. J Ecol Eng 2023:24. https://doi.org/10.12911/22998993/162984.
[2] Paulus N, Lemort V. Pollutant testing (NOx, SO2 and CO) of commercialized micro-combined heat and power (mCHP) fuel cells. https://doi.org/10.52202/069564-0104.
[3] Davila C, Paulus N, Lemort V. Experimental investigation of a Micro-CHP unit driven by natural gas for residential buildings. Proceedings of the 19th International Refrigeration and Air Conditioning Conference (Herrick 2022) 2022.
[4] Hoskins RF. Chapter 4 - Time-invariant Linear Systems. Delta Functions. Woodhead Publishing; 2011. p. 76–98. https://doi.org/10.1533/9780857099358.76.
[5] Baldi S, Le QT, Holub O, Endel P. Real-time monitoring energy efficiency and performance degradation of condensing boilers. Energy Convers Manag 2017;136:329–39. https://doi.org/10.1016/j.enconman.2017.01.016.
[6] Bennett G, Elwell C. Effect of boiler oversizing on efficiency: a dynamic simulation study. Build Serv Eng Res Technol 2020;41(6):709–26. https://doi.org/10.1177/0143624420927352.
[7] Paulus N, Lemort V. Grid-impact factors of field-tested residential Proton Exchange Membrane Fuel Cell systems. https://doi.org/10.34641/CLIMA.2022.176.
[8] Ghenciu AF. Review of fuel processing catalysts for hydrogen production in PEM fuel cell systems. Curr Opin Solid State Mater Sci 2002;6:389–99. https://doi.org/10.1016/S1359-0286(02)00108-0.
[9] Braun RJ, Klein SA, Reindl DT. Evaluation of system configurations for solid oxide fuel cell-based micro-combined heat and power generators in residential applications. J Power Sources 2006;158:1290–305. https://doi.org/10.1016/J.JPOWSOUR.2005.10.064.
[10] Dolci F, Thomas D, Hilliard S, Guerra CF, Hancke R, Ito H, et al. Incentives and legal barriers for power-to-hydrogen pathways: An international snapshot. Int J Hydrogen Energy 2019;44(23):11394–401. https://doi.org/10.1016/J.IJHYDENE.2019.03.045.
[11] Boait PJ, Greenough R. Can fuel cell micro-CHP justify the hydrogen gas grid? Operating experience from a UK domestic retrofit. Energ Buildings 2019;194:75–84. https://doi.org/10.1016/J.ENBUILD.2019.04.021.
[12] Paulus N, Job N, Lemort V. Investigation of degradation mechanisms and corresponding recovery procedures of a field-tested residential cogeneration Polymer Electrolyte Membrane fuel cell. To Be Submitted 2023.
[13] Zhang B., Wang L., Li R. Chapter 10 - Bioconversion and Chemical Conversion of Biogas for Fuel Production. Advanced Bioprocessing for Alternative Fuels, Biobased Chemicals, and Bioproducts: Technologies and Approaches for Scale-Up and Commercialization. Woodhead Publishing; 2019. p. 187–205. https://doi.org/10.1016/B978-0-12-817941-3.00010-3.
[14] Daoud I. Installer une Cogénération dans votre Etablissement. Ministère de La Région Wallonne Direction Générale Des Technologies, de La Recherche et de l'Energie (GGTRE) 2003.
[15] Korotkikh O, Farrauto R. Selective catalytic oxidation of CO in H2: fuel cell applications. Catal Today 2000;62:249–54. https://doi.org/10.1016/S0920-5861(00)00426-0.
[16] Wakita H, Kani Y, Fujihara S, Ukai K, Maenishi A. Hydrogen generator, fuel cell system and their operating methods. US8652224B2 2014. https://patentimages.storage.googleapis.com/11/ab/c7/703e1eb83a1a8c/US8652224.pdf.
[17] Adams WA, Blair J, Bullock KR, Gardner CL. Enhancement of the performance and reliability of CO poisoned PEM fuel cells. J Power Sources 2005;145:55–61. https://doi.org/10.1016/J.JPOWSOUR.2004.12.049.
[18] Valdés-López VF, Mason T, Shearing PR, Brett DJL. Carbon monoxide poisoning and mitigation strategies for polymer electrolyte membrane fuel cells – A review. Prog Energy Combust Sci 2020;79:100842. https://doi.org/10.1016/J.PECS.2020.100842.
[19] Zhang Y, Chen S, Wang Y, Ding W, Wu R, Li Li, et al. Study of the degradation mechanisms of carbon-supported platinum fuel cells catalyst via different accelerated stress test. J Power Sources 2015;273:62–9. https://doi.org/10.1016/J.JPOWSOUR.2014.09.012.
[20] Xie J, Wood DL, More KL, Atanassov P, Borup RL. Microstructural Changes of Membrane Electrode Assemblies during PEFC Durability Testing at High Humidity Conditions. J Electrochem Soc 2005;152:A1011. https://doi.org/10.1149/1.1873492/XML.
[21] Darling RM, Meyers JP. Kinetic Model of Platinum Dissolution in PEMFCs. J Electrochem Soc 2003;150:A1523. https://doi.org/10.1149/1.1613669/XML.
[22] European Commission. EN13757-4: Communication systems for meters and remote reading of meters - Part 4: Wireless meter readout (Radio meter reading for operation in SRD bands). 2013.
[23] Butler D, Abela A, Martin C. Heat meter accuracy testing. UK Government - Department for Business, Energy & Industrial Strategy; 2016. https://assets.publishing.service.gov.uk/government/uploads/system/uploads/attachment_data/file/576680/Heat_Meter_Accuracy_Testing_Final_Report_16_Jun_incAnxG_for_publication.pdf.
[24] International Organization of Legal Metrology. OIML R 75-1: 2002 (E): Heat meters Part 1: General requirements Compteurs d'énergie thermique Partie 1: Exigences générales. 2002.
[25] International Electrotechnical Commission. IEC 62053-21: Electricity metering equipment (a.c.) – Particular requirements. Part 21 : Static meters for active energy (classes 1 and 2). 2003.

[26] Paulus N, Lemort V. Establishing the energy content of natural gas residential consumption : example with Belgian field-test applications. IOP Conf Ser Earth Environ Sci 2023;1185:012013. https://doi.org/10.1088/1755-1315/1185/1/012013.
[27] Paulus N, Lemort V. Field-test performance of Solid Oxide Fuel Cells (SOFC) for residential cogeneration applications. Proceedings of the 7th International High Performance Buildings Conference at Purdue (Herrick 2022) 2022.
[28] European Parliament. DIRECTIVE 2010/31/EU on the energy performance of buildings. Official Journal of the European Union 2010.
[29] De Bruijn FA, Dam VAT, Janssen GJM. Review: Durability and Degradation Issues of PEM Fuel Cell Components. Fuel Cells 2008;8:3–22. https://doi.org/10.1002/FUCE.200700053.
[30] Paulus N, Davila C, Lemort V. Field-test economic and ecological performance of Proton Exchange Membrane Fuel Cells (PEMFC) used in micro-combined heat and power residential applications (micro-CHP). https://doi.org/10.11581/dtu.00000267.
[31] Staffell I, Green R, Kendall K. Cost targets for domestic fuel cell CHP. J Power Sources 2008;181:339–49. https://doi.org/10.1016/J.JPOWSOUR.2007.11.068.
[32] Orr G, Lelyveld T, Burton S. Final Report: In-situ monitoring of efficiencies of condensing boilers and use of secondary heating. Energy Saving Trust 2009. https://assets.publishing.service.gov.uk/government/uploads/system/uploads/attachment_data/file/180950/In-situ_monitoring_of_condensing_boilers_final_report.pdf.
[33] MathWorks. Matlab R2023a - Curve Fitting Toolbox User's guide. 2023.
[34] Zhang L, Xia J, Thorsen JE, Gudmundsson O, Li H, Svendsen S. Technical, economic and environmental investigation of using district heating to prepare domestic hot water in Chinese multi-storey buildings. Energy 2016;116:281–92. https://doi.org/10.1016/J.ENERGY.2016.09.019.
[35] Van Kenhove E, Dinne K, Janssens A, Laverge J. Overview and comparison of Legionella regulations worldwide. Am J Infect Control 2019;47:968–78. https://doi.org/10.1016/J.AJIC.2018.10.006.
[36] Paulus N, Davila C, Lemort V. Correlation between field-test and laboratory results for a Proton Exchange Membrane Fuel Cell (PEMFC) used as a residential cogeneration system. Annuel de La Société Française de Thermique" (SFT 2022); 2022. https://doi.org/10.25855/SFT2022-119.
[37] European Commission. Commission. Delegated Regulation No 811/2013 of 18 February 2013 with regard to the energy labelling of space heaters. ... Off J Eur Union 2013. https://eur-lex.europa.eu/legal-content/EN/TXT/PDF/?uri=CELEX:32013R0811&from=EN.